ELSEVIER

Journal of Hazardous Materials 45 (1996) 1–25

JOURNAL OF HAZARDOUS MATERIALS

Investigations to improve and assess the accuracy of computational fluid dynamic based explosion models

N.R. Popat[a,*], C.A. Catlin[a], B.J. Arntzen[b], R.P. Lindstedt[c], B.H. Hjertager[d], T. Solberg[d], O. Saeter[d], A.C. Van den Berg[e]

[a] *British Gas, Research and Technology, Gas Research Centre, Ashby Road, Loughborough, Leicestershire LE11 3QU, UK*

[b] *Christian Michelsen Research, Fantoft, Norway*

[c] *Imperial College of Science, Technology and Medicine, London, UK*

[d] *Telemark Technological Research and Development Centre, Porsgrun, Norway*

[e] *TNO Prins Maurits Laboratory, Rijswijk, Netherlands*

Received 10 August 1994; accepted 22 March 1995

Abstract

A summary is given of part of the CEC co-sponsored project MERGE (Modelling and Experimental Research into Gas Explosions). The objective of this part of the project was to provide improved Computational Fluid Dynamic explosion models with the potential for use in hazard assessments. Five organisations with substantial experience in both theoretical and experimental explosion modelling contributed to this model assessment study; British Gas, Christian Michelsen Institute, Imperial College, Telemark Technological Research and Development Centre and TNO Prins Maurits Laboratory. The theoretical and numerical basis of the models are described. Results are given of a comparison exercise of model predictions against calculations which were chosen to test the accuracy of the various physical sub-models embodied within the overall explosion model. The development phase of the study is also described in which further extensions to the models were made to provide the best achievable agreement with small- and medium-scale experiments also conducted as part of the project. The models were finally used to simulate large-scale explosion experiments prior to the experiments being conducted. The overall capabilities of the models are reviewed and areas of uncertainty in the physics highlighted.

Keywords: Computational fluid dynamics; Explosion models

1. Introduction

The Major Technological Hazards Programme of the Commission of European Communities (CEC-DGXII) has an objective to improve industrial safety. This is

* Corresponding author. Tel.: (44) 509 282442; Fax: (44) 509 2831119.

SSDI 0304-3894(95)00042-9

achieved by co-sponsoring projects involving groups of research organisations on the condition that the key findings are openly published, and any new technologies that are developed in the course of the work are made available to the public via publication and consultancy. This paper reports the results of the Computational Fluid Dynamic (CFD) modelling studies which formed part of project MERGE (Modelling and Experimental Research into Gas Explosions). The rapidly growing computational speed of modern computers is resulting in increasing usage of the CFD predictive method to simulate general, full-scale explosion scenarios. The method, being based upon fundamental descriptions of the governing physics, potentially provides the most accurate theoretical predictive technique for studying full-scale explosion behaviour which, at the large industrial scales of relevance, can be impractical to study experimentally.

A rapidly growing number of CFD explosion models are being used in explosion assessments. Each model, however, has been developed independently using different physical assumptions and, in particular, different sets of explosion data have been used to assess predictive accuracy. The objective of this study was to provide a critical comparison of the models, both in forms of the fundamental assumptions employed and in their predictive accuracy. Accuracy tests involved a range of verification calculations as well as simulations of a set of geometrically similar small-, medium- and large-scale experiments which were performed as part of the project. One specific explosion geometry, illustrated in Fig. 1, was used at all scales in which a flame accelerates through a regular array of obstacles. Ignition was by spark in a homogeneous fuel–air mixture which was initially quiescent. An unbiased test of the ability of the models to predict the change in explosion behaviour with the increasing size of the experiment was achieved in the following way. Only the small- and medium-scale experimental data were made available to the modellers for model development. Simulations of the large-scale experiments were then performed in advance of the experiments being conducted.

Five organisations of the eight involved in project MERGE contributed to this study. These were British Gas Research and Technology (BG), United Kingdom, Christian Michelsen Research (CMR), Norway, the Mechanical Engineering Department of Imperial College of Science, Technology and Medicine (ICSTM), United Kingdom, Telemark Technological Research and Development Centre (Tel-Tek), Norway, and TNO Prins Maurits Laboratory (PML), Netherlands. PML provided overall co-ordination of the project. All organisations have their own CFD explosions code. Tel-Tek [1] and Christian Michelsen Research [2] use the EXSIM and FLACS codes, respectively. PML have recently developed the REAGAS code [3] which has a similar basis to that of EXSIM. BG were making their first application to explosions of the COBRA code (a software product of Mantis Numerics Ltd.). These four codes are all being developed for the purpose of simulating realistic explosion scenarios, and as such require additional 'sub-models' to describe those physical processes which occur at scales below the resolution of the computational grid. The sub-models, in particular, must represent the effects that the obstacles have on the flow, turbulence and the flame. In contrast ICSTM, using the GEISHA code (a software product of Computational Dynamics Ltd.), conducted fine resolution calculations, in which the

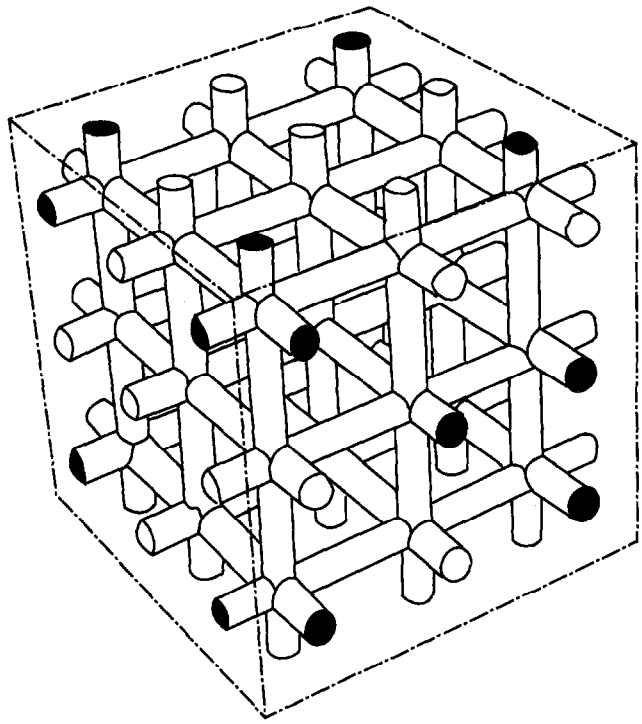

Fig. 1. Illustration of geometry used in experimental and theoretical explosion studies.

bodies were grid-resolved. These results provided data for evaluating the plausibility of the sub-modelling assumptions used in the other codes.

This paper describes the model comparison study which was conducted in two parts. The first was a verification exercise in which a range of idealised calculations were defined to test the accuracy of both the codes and the individual physical sub-models. The second was the development stage, in which the models were extended with the aim of obtaining accurate predictions of both the small- and medium-scale experimental data. These improved models were finally used to simulate the large-scale experiments prior to their being conducted. This paper starts with a basic description of the different models and concludes with a discussion of the results and areas of uncertainty.

2. Experimental work

The modelling studies to be described below were all aimed at the final objective which was to simulate the experiments (see Ref. [4] for details) also being conducted as a part of the MERGE project. Medium- and large-scale experiments were conducted by BG and small-scale experiments by PML. The medium- and large-scale data were principally used to validate the models and are briefly summarised below.

The medium-scale geometry is shown in Fig. 2, in which the obstacles occupy a cuboidal region 2.0 m high with a 4.0 m^2 base. This was enclosed in polythene sheet (4.5 m × 4.5 m × 2.25 m) to contain the flammable gas. The ignition point was adjacent to the floor and central to the base region of the obstacles. This resulted in an accelerating hemi-spherical flame. The flame position was determined from cine film

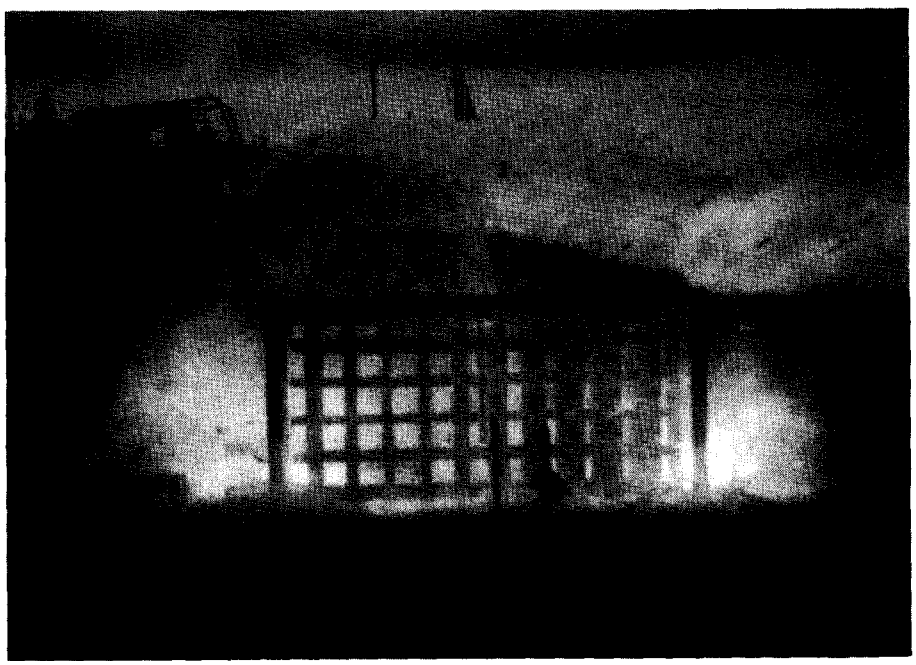

Fig. 2. An explosion within a medium-scale MERGE experimental geometry.

Table 1
Summary of tests conducted as part of project MERGE: rig types A–D are medium-scale (obstacles 4 m × 4 m × 2 m high), rig types E and C* are large-scale (obstacles 8 m × 8 m × 4 m high)

Type	No. of tests	Pitch P (m)	Diameter D (m)	Volume blockage (%)	Fuel[a] type
A	7	0.200	0.043	10	M, P, E, Mx, OM, OP, OMx
B	4	0.133	0.041	20	M, P, E, Mx
C	4	0.400	0.086	10	M, P, E, Mx
D	7	0.267	0.082	20	M, P, E, Mx, OM, OP, OMx
E	3	0.800	0.168	10	M, P, Mx
C*	3	0.384	0.082	10	M, P, Mx

[a] M = methane/air, P = propane/air, E = ethylene/air, Mx = methane:propane mix (volume ratio 3:1)/air, OM = methane/oxygen-enriched air, OP = propane/oxygen-enriched air, OMx = methane:propane mix/oxygen-enriched air.

together with flame detectors placed within the obstacles. The pressure wave was measured using pressure transducers placed on the ground at various distances along a radial line from the ignition point. The large-scale geometry had approximately twice the linear dimensions of the medium-scale.

The test conditions for the medium- and large-scale experiments are summarised in Table 1. There were six types (A, B, C, D, E, C*) of obstacles in all, each characterised by the pipe diameter (D) and pitch (P – shortest distance between the centres of adjacent pipes). Their volume blockages were either 10% or 20%. Four obstacle types (A, B, C, D) were used at medium-scale and two, E and C*, at large-scale. These are scaled-up equivalents of C and A, respectively.

All of the flammable atmospheres were stoichiometric mixtures of hydrocarbons (methane, propane and ethylene) and air, or oxygen-enriched air (See Table 1).

3. Mathematical modelling

3.1. Equations solved and numerical approaches

As the basic form of the equations for the turbulent explosion problem have been well documented previously [5] it is sufficient here to describe the differences between the theoretical and numerical formulations of the models. Essentially all the codes solve for conservation of mass, momentum and energy. The energy equation has been formulated and solved in terms of enthalpy in EXSIM, FLACS and REAGAS. The COBRA code solves for total energy (internal plus kinetic). The codes employ different numerical techniques, COBRA being based on a second-order (in time and space) explicit Godunov method [6] and the others on the hybrid scheme incorporated into the SIMPLE pressure-correction method applied to compressible flows [7]. The flame is modelled in the codes by solving for a reaction progress variable. FLACS differs from EXSIM and REAGAS, however, by applying the second-order Van Leer scheme [8] to the reaction progress variable equation. The lower numerical diffusion of this scheme enables the flame to be resolved using fewer computational cells than required by the hybrid scheme. All codes employ the standard k–ε turbulence model [9]. The other main difference relates to the computational grids employed. EXSIM, FLACS and REAGAS all use fixed grids, the momentum equations being solved on a staggered grid as is conventional with the SIMPLE pressure-correction technique. The COBRA code has been implemented with an adaptive grid based on a nodal embedding strategy [10] which enables the grid to refine automatically in regions where greater resolution is required, such as the flame. Although GEISHA was not used in the code comparison exercise it is worth recording that the program uses a second-order TVD scheme [11] implemented in a version of the PISO algorithm [12].

3.2. Physical sub-models

Even with the capacity of modern-day computers, it is still not possible to resolve all of the physical processes involved in a realistic full-scale explosion scenario on the

computational grid. This is because of the very large difference in scale between the region of influence of the explosion, and the relatively very much smaller structures within the flame and the wakes of the obstacles. In order to apply CFD to realistic scenarios, therefore, it is necessary to develop approximate mathematical descriptions of the small-scale physical processes which cannot be resolved on the computational grid. These are given the generic name 'sub-grid' models in the following.

3.2.1. Sub-grid drag and turbulence

Conventionally drag and turbulence effects [5] were modelled by the inclusion of source terms in the momentum (S_u) and turbulence kinetic energy (S_k) equations, respectively:

$$S_{ui} = -C_d \cdot \tfrac{1}{2}\rho |u_i| u_i,$$

$$S_k = +C_k \cdot C_d \cdot \tfrac{1}{2}\rho |u_i|^3,$$

where ρ and u_i are the gas density and velocity, respectively.

The form of the drag source term, which amounts to a 'sink' in the momentum equation, is based upon the familiar expression for incompressible steady flows ($A = C_d \cdot \frac{1}{2}\rho u^2$). The turbulence kinetic energy source was taken to be a fraction of the energy loss associated with the momentum loss, C_k, therefore taking a value between 0 and 1. A value of 1 assumes that the entire energy loss from the mean flow, which is caused by drag, manifests itself as turbulence kinetic energy. The turbulence constant C_k is generally assumed to be independent of the obstacle type. The values of C_k assumed in the models, however, differ (see Table 2). Different drag constants (C_d) were also assigned to each type of obstacle. The values used in the verification study described below are summarised in Table 2 together with Refs. [13–16] to the sources of data. It is noted that in the validation part of the study some modellers needed to use drag constants which were different from these in order to get consistent agreement with the explosion experimental data.

Table 2
Drag and turbulence modelling constants used in verification exercise (P is pitch, D is pipe diameter)

Organisation	C_k	L (m)	C_d Obstacle type					
			A	B	C	D	E	C*
Tel-Tek [13]	0.3	0.12D	0.48	1.08	0.24	0.54	0.12	0.25
CMR [14]	0.5	0.1D	0.91	1.87	0.41	0.82	0.18	0.43[a]
			0.69	1.42	0.31	0.62	0.14	0.33[b]
PML [15]	0.5	0.1P	0.90	2.00	0.40	1.00	0.20	0.40
BG [16]	1.0	0.1P	0.69	1.70	0.35	0.85	0.18	0.43

CMR developed a velocity-dependent drag model such that (a) has 50 m/s velocity and (b) has 200 m/s velocity.

In all of the models, the turbulence length-scale (L) in the sub-grid region was imposed, as opposed to being modelled. This imposed value of L (m) was typically either a fraction of the obstacle diameter or pitch (see Table 2). The value of the turbulence dissipation rate (ε; m^2/s^3) was computed from the local value of turbulence kinetic energy (k; m^2/s^2), using the familiar expression [1]

$$\varepsilon = C_\mu^{3/4} k^{3/2}/L.$$

In regions without obstacles the turbulence length scale L was inferred from the k–ε equations using the above expression.

3.2.2. Ignition and laminar flame propagation

Independent work [17] has established that there must be at least 5 computational cells in the flame zone before an accurate solution is achieved within the reaction zone. Thus, in order to mimic the flow field generated by the early and very thin laminar flame, all of the explosion models make a correction to the reaction rate. A single multiplying factor was applied to the reaction rate in each computational cell to ensure that the sum total of the reaction rates in all cells equated to that of a spherical flame with a specified flame speed (or, equivalently, burning rate). This method can be readily implemented in fixed grid codes. In order to implement this procedure in the adaptive grid code it was necessary to 'freeze' the adaptive finite-volume procedure in the immediate vicinity of the ignition point. This correction procedure was relaxed once the flame had grown to sufficiently large a radius for the flame to be resolved adequately on the grid.

The laminar burning rate during this phase was prescribed in different ways in the various models. Most assigned well-documented values [18] to the fundamental laminar burning velocity which was then multiplied by an enhancement factor (E_L) to account for wrinkling of the flame front. Wrinkling occurs because of natural instabilities or as a result of interaction of a flame with obstacles. E_L is typically a function of the flame radius R (m) (see Table 3).

3.2.3. Turbulent flame propagation

The burning velocity of the turbulent flame (the burning velocity is the velocity of the flame relative to the unburned reactants or, equivalently, the rate at which the flame consumes unburned reactants) is determined by the turbulent reaction rate and the corresponding turbulent viscosity [17] in the equation for the reaction progress variable. Tel-Tek and PML took the longest established approach [19, 1] of prescribing a turbulent reaction rate (R_{fu}) in terms of an eddy break-up model. ICSTM employed a new formulation of the eddy break-up model [20] which was developed in the course of the project.

CMR and BG took a different approach by defining the reaction rate and turbulent viscosity in the reaction progress variable equation so as to ensure the flame had the turbulent burning velocity prescribed by an empirical correlation. The CMR and BG approaches do not take account of the effects of turbulent quenching whilst the

Table 3
Laminar flame area enhancement factor E_L and turbulent flame area enhancement factor E_T (R is radial distance of the flame from the ignition point, E is expansion ratio, P is pitch, D is pipe diameter, A denotes calibrated constants)

Organisation	
Tel-Tek	$E_L = \min(1 + 4R, 3)$ $E_T = 1.0$
CMR	$E_L = \max[\min(R/P, 2), 1]$ $E_T = \max[(R/P)^{0.4}, 1]$
PML	$E_L = (1 + AR)$ $E_T = A$
BG	$E_L = \exp(AR/P)$ $E_T = 1 + ED/P$

approach of Tel-Tek and PML has been specifically developed to include the effects of turbulent quenching (see below).

In order to achieve accurate solutions when using the latter method to prescribe the burning rate it is necessary to establish a minimum number of computational cells in the flame zone [17]. As FLACS uses a fixed grid, CMR employed the 'β-transformation' method [21,22] to control the flame thickness to ensure the flame zone occupied sufficiently many computational cells. BG on the other hand assigned the flame thickness on physical criteria and used the adaptive grid in COBRA to ensure the reaction zone remained sufficiently grid-resolved. Since the Tel-Tek and PML codes solve fundamental equations for the reaction zone, flame thickness is not controlled. The size of the computational cells must, therefore, be chosen sufficiently small to ensure grid resolution of the reaction zone. This is not necessarily a major constraint since the conventional eddy break-up models naturally predict a thick flame.

The details of the turbulent reaction models are as follows:

Tel-Tek and PML (Ref. [23])

This model takes account of turbulence by setting the reaction rate (R_{fu}) to zero in regions where the ratio of turbulence (τ_{tu}) and chemical (τ_{ch}) time scales exceeds some critical value (D_{ac}). Therefore,

$$R_{fu} = -A \cdot \rho \cdot \varepsilon/k \cdot Y_{lim} \quad \text{if } D_a < D_{ac}$$

or

$$R_{fu} = 0 \quad \text{if } D_a > D_{ac},$$

where

$$D_a = \tau_{ch}/\tau_{tu}, \quad D_{ac} = 1000,$$

$$\tau_{ch} = A_{ch} \cdot \exp(E/RT) \cdot (\rho Y_{fu})^a \cdot (\rho Y_{ox})^b, \quad \tau_{tu} = \varepsilon/k.$$

Here Y_{lim} is the minimum of the mass fractions of fuel (Y_{fu}), oxygen (Y_{ox}/s) or fuel already burned ($Y_{fu,b}$), s is the stoichiometric oxygen required to burn 1 kg of fuel, T is the absolute temperature, A_{ch}, a and b are chemical rate constants, E and R are the activation energy and universal gas constant, respectively, and A is combustion model constant.

CMR (Refs. [24, 25])

The turbulent burning velocity is given as the minimum of two correlations for low and high turbulence levels due to an analysis of the experimental data in Ref. [24] and that due to Bray [24], respectively:

$$u_t = \min(u_t^{low}, u_t^{high}),$$

where

$$u_t^{low} = u_l + 8u_l^{0.284}u'^{0.912}L^{0.196},$$

$$u_t^{high} = 15u_l^{0.784}u'^{0.412}L^{0.196}$$

and u_l and u' are the laminar burning velocity and root mean square (r.m.s.) of the turbulent velocity fluctuations, respectively.

BG (Ref. [24])

The expression provided below is a correlation to the turbulent burning velocity measurements of the Leeds University Mechanical Engineering group provided by Bray [24]:

$$u_t/u_l = 0.875K^{-0.392}u'/u_l,$$

where

$$K = 0.157(u'/u_l)^2/\sqrt{R},$$

and Re is the turbulent Reynolds number ($u'L/v$) and is equivalent to u_t^{high} above.

4. Model verification

The correctness of the numerical and physical sub-modelling approaches used was established by obtaining numerical solutions to a range of simple flow problems to which the exact solutions are known. Such problems include predicting the shock and rarefaction waves generated in the classical Riemann or 'shock tube' problem [26], as well as the Blasius profile of the developing planar shear layer [27]. Such problems provided independent tests of the models' accuracy for studying transient gas dynamics, including the resolution of shock waves and contact surfaces, and the effects of viscosity.

For the explosion problem, however, it is necessary to extend the verification to include tests of the individual sub-models. Both steady flow and transient flow problems were formulated to test the principal sub-models, namely those for drag, turbulence and turbulent burning rate, as described below.

The ignition sub-models were also tested for the case of a one-dimensional planar flame propagating away from a closed boundary. In this case, by virtue of the way they are implemented, all demonstrated by ability to establish quickly a flame speed which was close that specified.

4.1. Sub-grid drag and turbulence

Solutions were obtained for the fluid and turbulence parameters for a one-dimensional flow through a 5 m extent of obstacles. Constant inlet flow velocities of 10, 50 and 200 m/s were prescribed for a steady flow case. In transient cases, these incident flow velocities were generated by shock waves (i.e. the 'inlet' velocities correspond to the particle velocities immediately behind the shock). In the transient case the reflected wave, generated by the shock's interaction with the sub-grid region representing obstacles, slows the incident flow field.

Unlike the transient problem, the steady flow problem has exact solutions which can be derived by integration of the governing ordinary differential equations. Solutions only exist, however, provided the flow velocities remain sub-sonic. The conditions under which the sonic condition (choking) occurred differed between the models because the drag coefficients differed. Chocking occurred at lower incident velocities for those models with larger drag coefficients.

In general, all of the models were able to predict the exact solutions but it was necessary to ensure that the grid cells were sufficiently small relative to the turbulent integral length scale which was imposed in the sub-grid region. Fig. 3 shows predictions of the EXSIM code for seven levels of grid refinement in which the 25 m long computational domain was represented by NX cells. The flow is in the positive X-direction and the obstacles occupy the region 5 m $< X <$ 10 m. All but the turbulence length scale predictions converge to a grid-independent solution. Clearly the region immediately downstream of the obstacles ($X >$ 10 m) is the most sensitive to grid refinement. This effect occurs in these particular simulations because of the very small (0.0065 m) turbulence length scale which has been assigned. Even for the finest grid (NX = 1282) the computational cell size (0.02 m) is too large to resolve the very steep spatial gradients in the turbulence parameters which occur immediately downstream of the obstacles. It was concluded that in order to achieve an accurate solution, the computational cells have to be of a similar size to the imposed integral length scale. The sizes of the computational cells required to obtain grid-independent solutions differed for the different models, the smallest cells being required for the smallest imposed turbulence length scales.

The solution to the transient, shock-induced, flow problem evolves smoothly towards steady solution. Fig. 4 shows predictions of the REAGAS code for the turbulence velocity and turbulence length scale as the shock passes through the domain.

4.2. Turbulent burning rate

As the different explosion codes employ very different approaches to modelling the turbulent flame there is no absolute test of accuracy. The relative accuracies of the

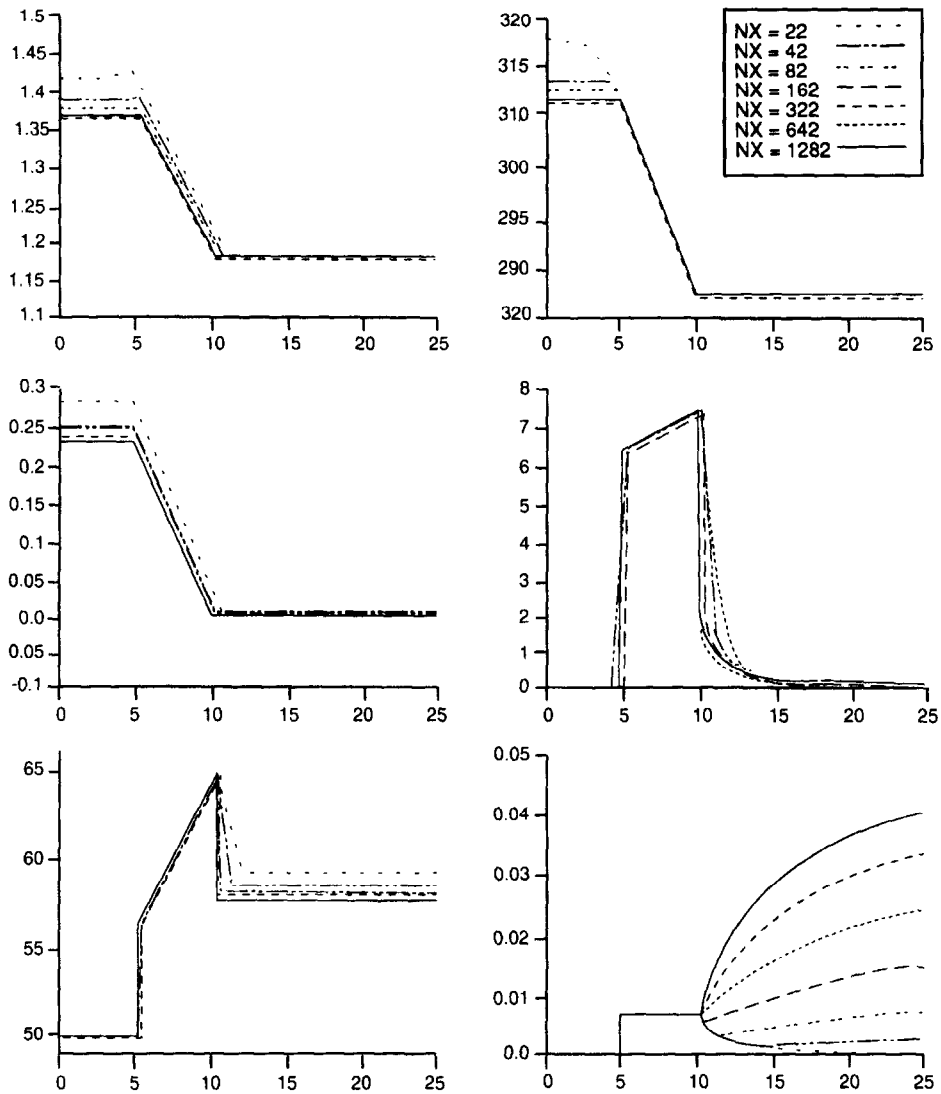

Fig. 3. Flow field and turbulence parameters [ordinate: (a) density (kg/m^3), (b) temperature (K), (c) overpressure (bar), (d) turbulent velocity (m/s), (e) flow velocity (m/s), (f) turbulent length scale (m); abscissa: coordinate X (m)] from the verification study for steady flows (Tel-Tek).

codes were therefore assessed by comparing predictions of burning velocity for a range of values of turbulence velocity and turbulence length scale against the empirical correlation [24] employed to prescribe turbulent burning velocity. As the explosion codes are designed to predict transient flows they all had to be modified to keep the turbulence parameters constant. Simulations were then performed of one-dimensional planar flames propagating away from a closed boundary, towards an

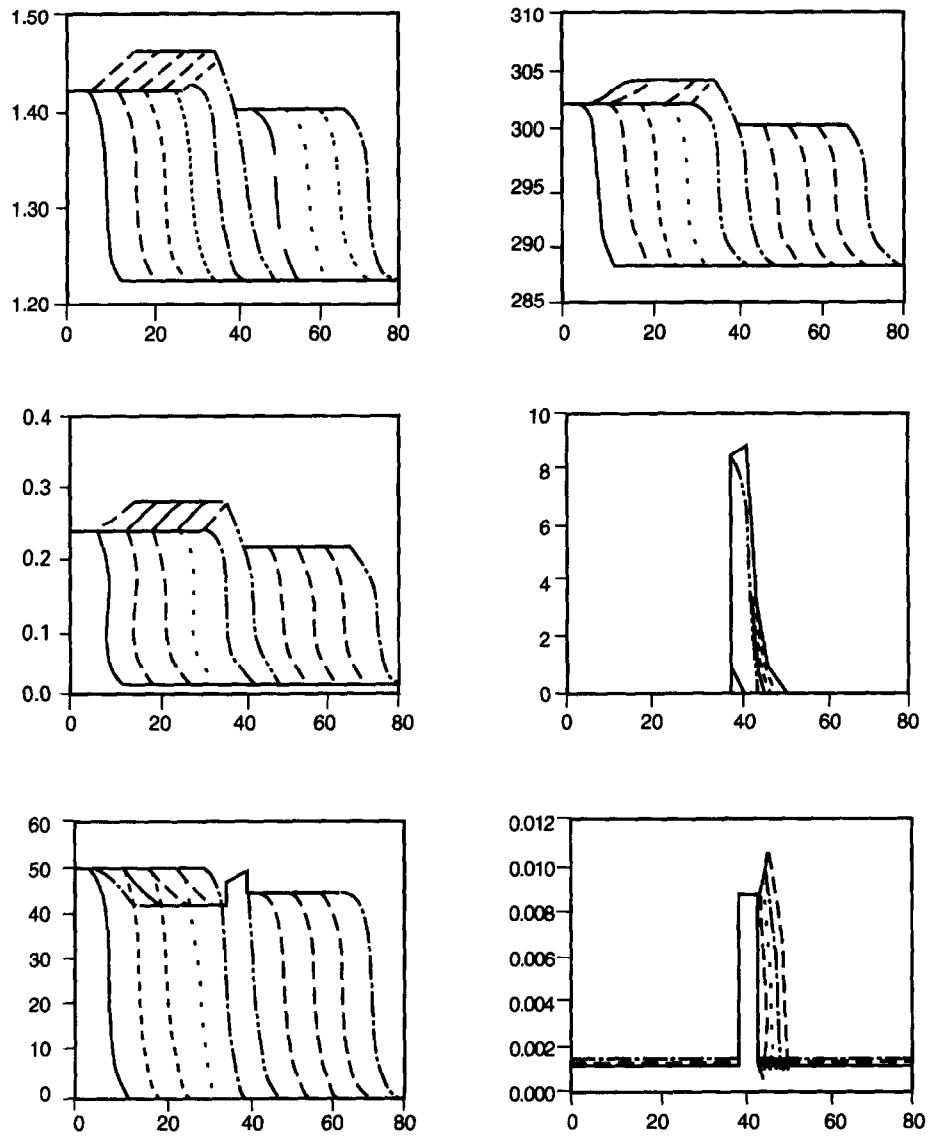

Fig. 4. Flow field and turbulence parameters [ordinate: (a) density (kg/m^3), (b) temperature (K), (c) overpressure (bar), (d) turbulent velocity (m/s), (e) flow velocity (m/s), (f) turbulent length scale (m); abscissa: coordinate X (m)] from the verification study for transient flows (PML).

open boundary, in a constant turbulence field. Once a steady flame speed had been achieved the burning velocity (u_t) was deduced from the particle velocity (u_p) immediately ahead of the flame using the relationship $u_t = u_p/(\rho_u/\rho_b - 1)$, where ρ_u and ρ_b are the densities of the unburned and burned gas, respectively.

Calculations were performed for stoichiometric mixtures in air of methane, propane and ethylene with spatially uniform r.m.s. turbulence velocities of 1, 5 and 50 m/s and turbulence length scales of 0.01, 0.04 and 0.10 m, typical of full-scale explosions. Results of these comparison calculations are summarised in Table 4 which show substantial differences between the Bray correlation [24] and the eddy break-up based combustion models of Tel-Tek and PML. In light of these substantial differences Tel-Tek developed a modified eddy break-up model to improve the predictive accuracy. These results are also shown in Table 4. The models of CMR and BG, by virtue of their design, were able to reproduce the correlations very closely.

In the accelerating flame calculations, the flame was simulated to propagate through a spatially varying turbulence field which increased from 5 to 50 m/s over a distance of 1.0 m and which remained constant at 50 m/s at larger distances again with constant turbulence length scales L of 0.01, 0,04 and 0.10 m. These calculations were designed specifically to test the ability of the codes to respond to the rapid changes in turbulence which may occur in the experiments. A linear ramp in turbulence parameters between $X = 0$ and $X = 1$ was defined by

$$u' = 5.0 \cdot \max(9X + 1, 10)$$

and the instantaneous relationship between burning velocity and turbulence predicted by the code compared against that given by the Bray correlation [24]. Example predictions from the FLACS, COBRA, EXSIM and REAGAS codes, for the case with L fixed to 0.01 m, are given in Fig. 5.

Table 4
Turbulent burning velocities predicted by the various combustion models

u' (m/s)	1	1	1	5	5	5	50	50	50
L (cm)	1	4	10	1	4	10	1	4	10
Bray[a]									
Methane–air	2.8	3.5	4.4	5.4	7.1	8.5	14	18	22
Propane–air	3.1	4.1	4.9	6.1	8	9.6	16	21	25
Tel-Tek									
Methane–air	0.54	0.57	0.59	2.5	2.7	2.8	23.6	26.0	27.8
Propane–air	0.60	0.64	0.68	2.8	3.0	3.2	27.5	30.6	32.7
Methane–air[b]	3.2	4.1	5.0	6.3	8.2	9.8	17.4	23.5	28.3
Propane–air[b]	3.7	4.9	5.9	7.3	9.7	11.6	19.7	26.9	32.7
PML									
Methane–air	0.88	0.90	0.93	4.0	4.2	4.3	32.0	33.0	34.0
Propane–air	0.96	0.98	1.0	4.4	4.6	4.8	35.0	36.0	37.0

[a] Empirical correlation to data of Bradley et al. (Ref. [23]), U_L (methane–air) = 0.37, U_L (propane–air) = 0.43.

[b] Predictions given using a modified eddy break-up combustion model.

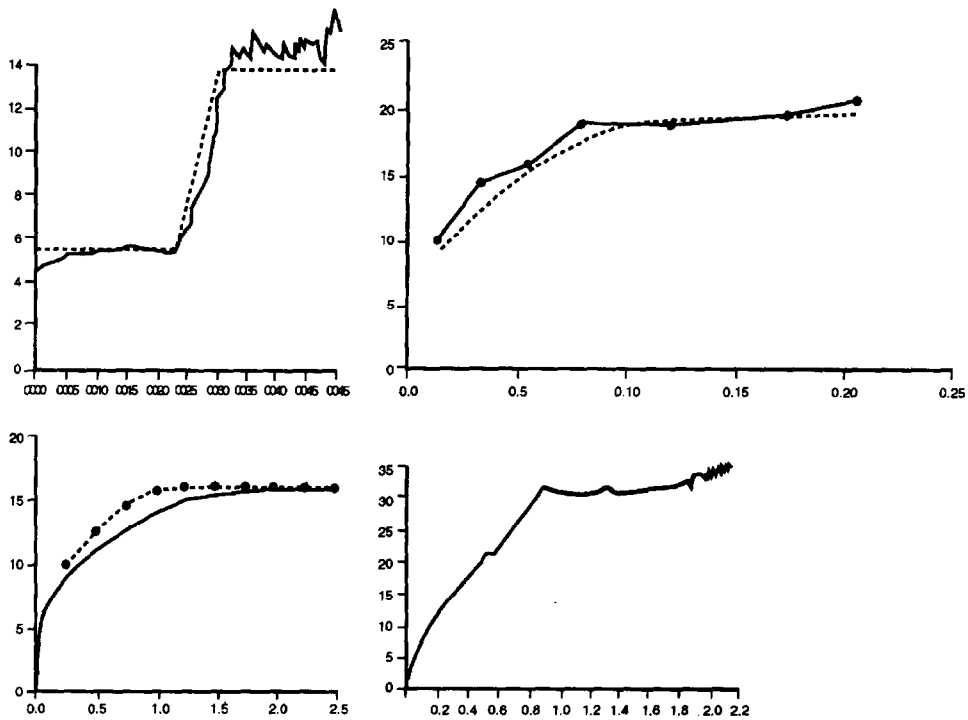

Fig. 5. Burning velocity for methane in a transient turbulent field: (a) CMR; (b) BG; (c) Tel-Tek; (d) PML. (····) experiment, (———) simulation.

5. Model development

The sub-models within the various codes were developed further in order to achieve good agreement between code predictions and the small- and medium-scale experiments. Even though great care was taken to implement valid sub-models during the verification exercise (based upon the best current understanding of the physics), several modellers found it necessary to introduce additional sub-models and/or sub-modelling parameters before the codes gave predictions which were consistent with the trends in the experimental data. As a result of this the MERGE project participants agreed to focus attention on developing sub-models for achieving good agreement for the positive phase of the pressure–time profiles of the small- and medium-scale experiments. The negative phase would then be modelled with sub-models as described above with no additional sub-models. The different groups, however, used different approaches which are summarised in Table 5.

Three of the models retained literature values of the drag coefficient (C_d) for steady flows. However, the sources of the information differed, Tel-Tek employing a drag formulation like that used for porous media [13] and PML based on a constant drag coefficient for circular tubes in steady cross flow. CMR used data obtained for flows

Table 5
Different modelling assumptions used in the validated codes

	Tel-Tek	CMR	PML	BG
C_d	Literature	Literature	Literature	Calibrated
Ignition	Laminar	Laminar	Laminar	Laminar
Turbulent combustion model	Modified eddy break-up	Bray + low r.m.s. correlation	Eddy break-up	Bray correlation
Turbulent flame area enhancement	No	Yes	Yes	Yes

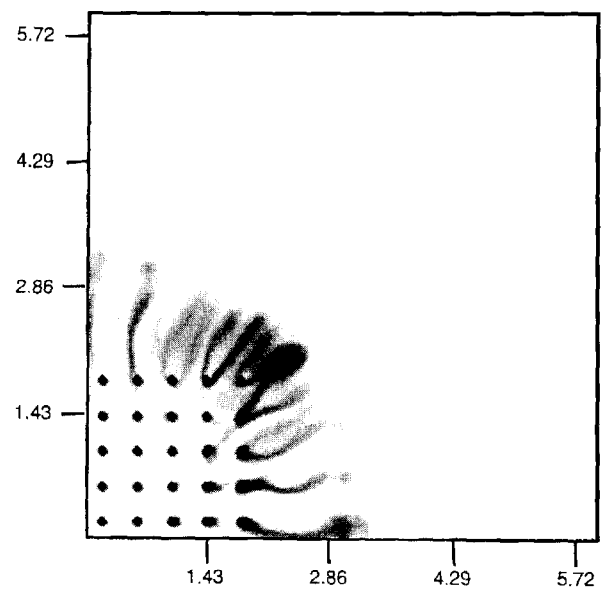

Fig. 6. Vortex structures predicted in fully resolved calculations – variations in turbulent kinetic energy are shown (ICSTM).

past rod bundles [15]. BG on the other hand introduced C_d values which were calibrated, to obtain agreement with experimental trends. The C_d values differ from the steady values used in the verification study, which BG suggest is due to the effects of flow development and transients. ICSTM suggest that their fully resolved calculations provide evidence for the role of transient flow processes. Fig. 6 shows vortex-like regions of high turbulence in the wakes of the bodies outside the region with obstacles.

For the ignition phase all four codes used laminar burning rates as specified in the validation studies.

The turbulent combustion models remained the same as those used in the verification exercise. PML, CMR and BG applied a burning rate enhancement factor (E_T) to

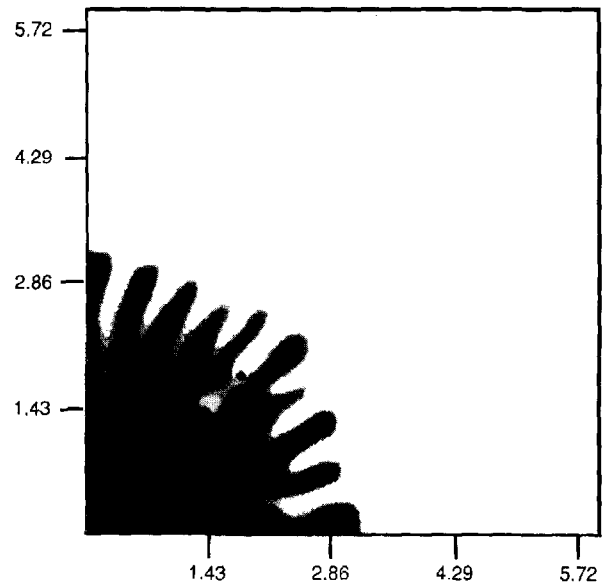

Fig. 7. Corrugation of turbulent flame front fully resolved calculations – variations in flame reaction progress variable are shown (ICSTM).

either the reaction rate in the eddy break-up model or to the burning velocity, to take account of the increase in the area of the flame caused by the flame's passage through the obstacles. Tel-Tek did not use a burning rate enhancement for the turbulent flame propagation.

This enhancement effect was not clearly observed in the film of the experiments but the very important role it plays in increasing the total burning rate can be seen in the 'grid-resolved' calculations of Fig. 7. The resolved calculations demonstrate that the higher flow velocities through the gaps between the obstacles cause the flame to develop 'fingers'. The fingering pattern and also the enhancement factor depend upon the obstacle geometry. PML and CMR used an empirical enhancement factor, whereas BG derived an approximate expression in terms of the pitch to diameter ratio of the obstacles, by assuming the flame has a constant burning velocity (see Table 3).

6. Model validation

As the development work aimed to ensure good agreement between the model predictions and the small- and medium-scale experiments, it is important to discuss the predictive accuracy of the models in an overall sense. It is mentioned here that comparison of model predictions with experimental data is not possible on a strictly ensemble-averaged basis, i.e. results obtained over a large number of experimental trials. This is because the experiments considered were expensive to perform, and hence only a limited number were carried out. There are many examples where the

model predictions agree remarkably well with experiment. Fig. 8 provides such an example, showing close similarity between the shapes of the predicted and measured pressure–time profiles, indicating that the predicted flame acceleration is close to that in the actual experiment.

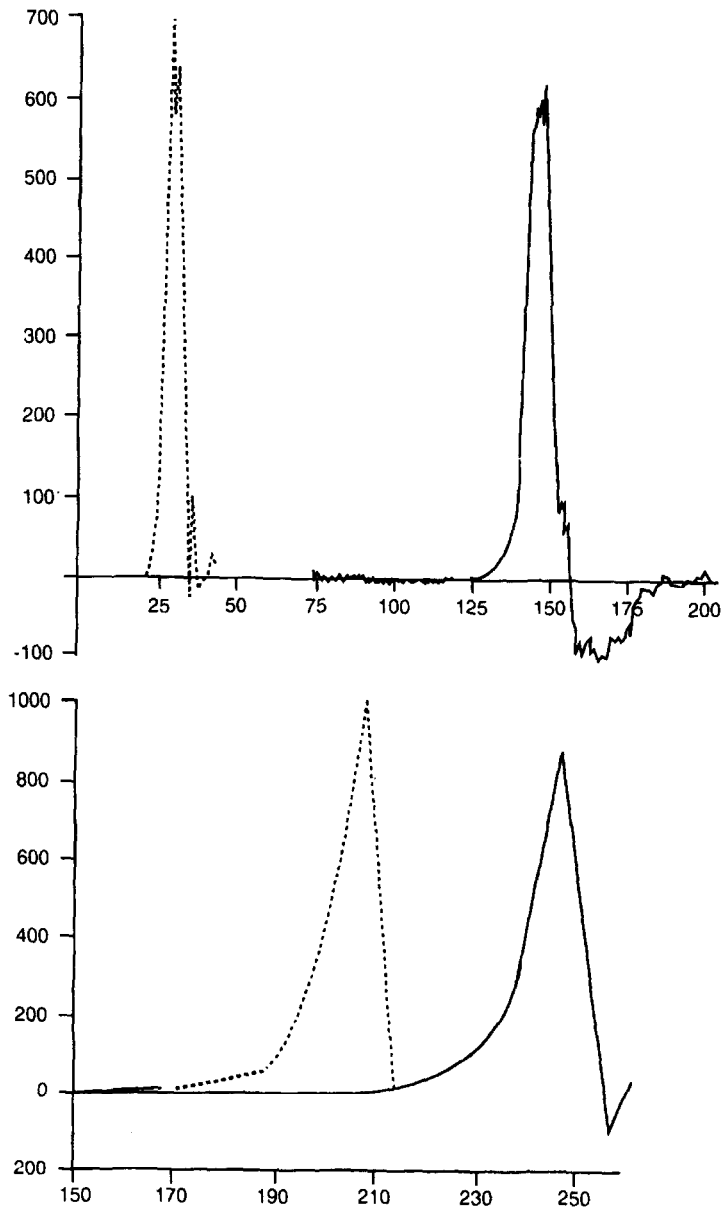

Fig. 8. Predicted and experimental overpressure–time profiles: (a) BG (methane, A); (b) CMR (methane, C*). Overpressure (mbar), time (ms). (·····) simulation, (———) experiment.

A global picture of accuracy, however, can only be obtained by comparing all predictions and experimental data. An example of such a scatter plot for all the medium-scale data supplied by BG and Tel-Tek, including experiments with the most reactive mixture (ethylene–air) which detonated, is provided in Fig. 9. The PML and CMR data have been excluded from these plots since the medium-scale experiments were used by these contributors as the primary means of calibrating their modelling constants. To include their results in the comparison would not, therefore, have provided a representative evaluation of the accuracy of their models. All but one experiment yielded results within a factor of two of the prediction. These results show the predicted peak overpressures are much more accurate when the experimental overpressures are below 1.5 bar (see Fig. 10). This suggests that the accuracy of the sub-models lessens at higher overpressures as the deflagration to detonation regime is

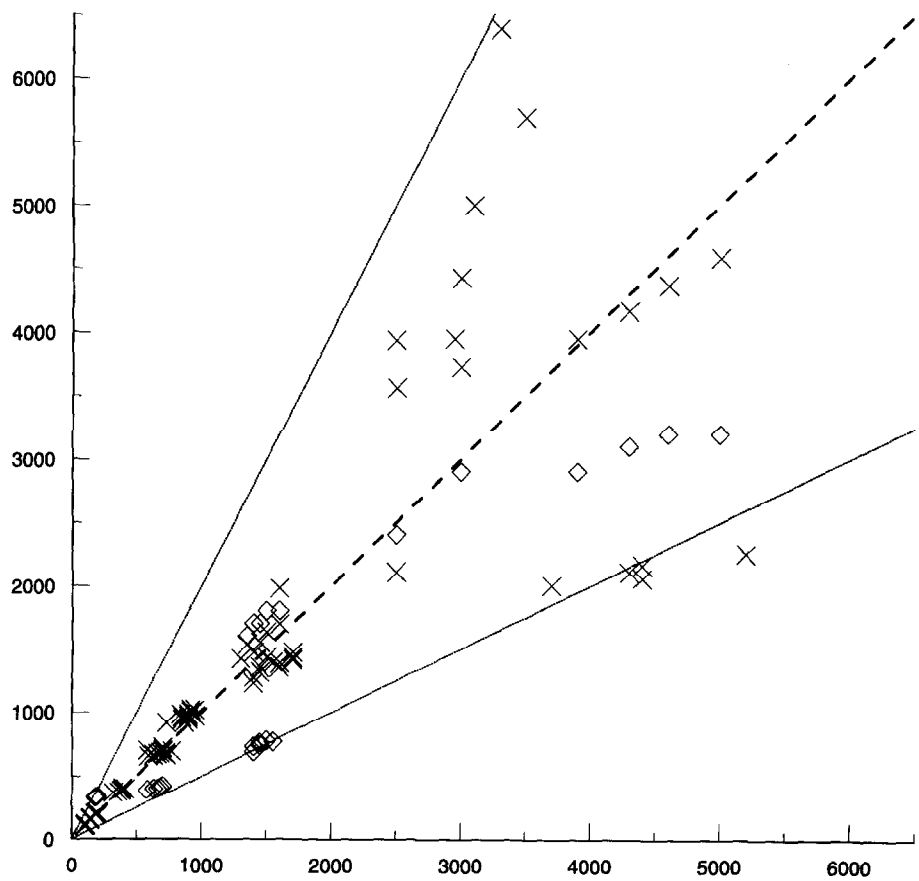

Fig. 9. Comparison of experiment and simulation for MERGE medium-scale experiments (BG, Tel-Tek). (×) COBRA predictions, (◇) EXSIM predictions. Simulated maximum overpressure and experimental maximum overpressure (mbar).

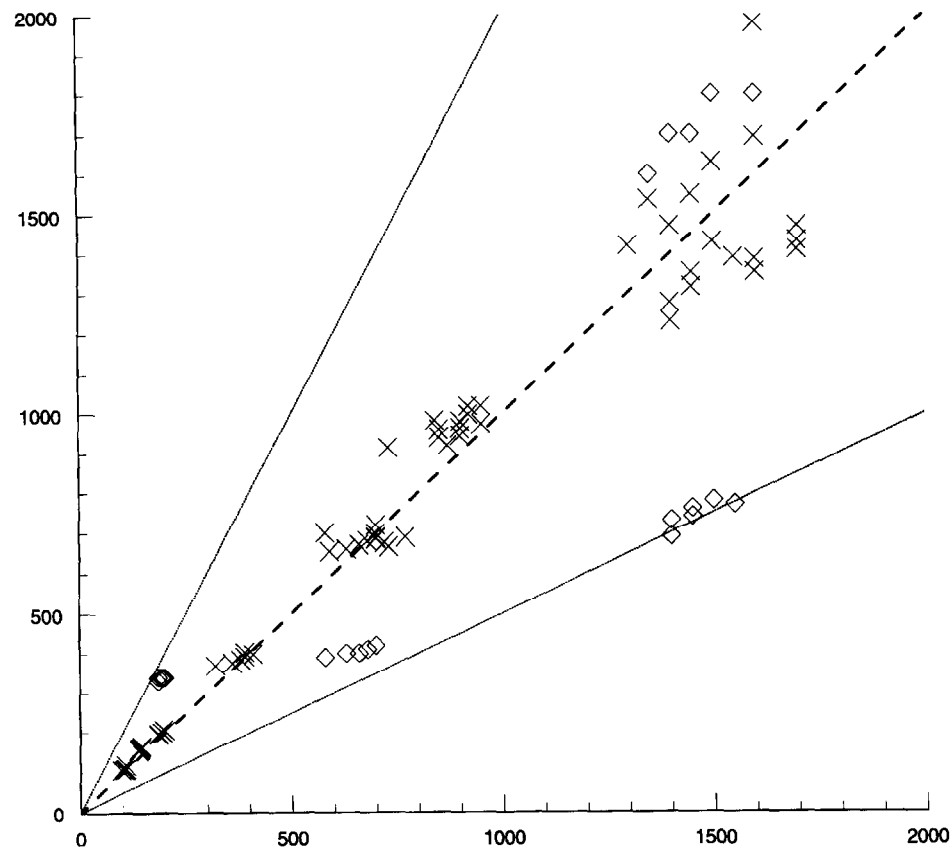

Fig. 10. Comparison of experiment and simulation for MERGE medium-scale experiments with peak overpressures below 1.5 bar (BG, Tel-Tek). (×) COBRA predictions, (◇) EXSIM predictions. Simulated maximum overpressure and experimental maximum overpressure (mbar).

entered. This result is not surprising, however, since the turbulent combustion model employed takes no account of the role that strong shocks play in the combustion process.

The second phase of the validation study concerned the a priori prediction of the large-scale experiments. The predictions are summarised in Table 6 in terms of the peak overpressure, the time of occurrence of the peak and the duration of the positive overpressure pulse.

It is immediately evident that the time of peak overpressure varies greatly and, in particular, the BG model consistently underpredicts this value. It should be noted, however, that the predominant part of this delay is taken up by the initial period of flame propagation when the flame is travelling at its slowest and not generating significant overpressures. Those models which treat the laminar phase accurately will therefore be able to accurately predict the time of occurrence of the peak overpressure.

Table 6
Summary of large-scale simulation results

Institute obstacle type/fuel	Maximum overpressure (mbar)	Time at maximum overpressure (ms)	Duration (ms)
Experiment			
E/methane	140	450	60
E/propane	230	390	60
C*/methane	850	250	27
C*/propane	2360	237	12
Tel-Tek			
E/methane	150	310	80
E/propane	430	260	50
C*/methane	540	270	40
C*/propane	2350	210	20
CMR			
E/methane	160	485	40
E/propane	300	425	30
C*/methane	900	210	20
C*/propane	1960	190	20
PML			
E/methane	170	600	50
E/propane	350	430	40
C*/methane	2900 (1030)[a]	361	15
C*/propane	4190 (2700)[a]	209	13
BG			
E/methane	165	115	30
E/propane	320	90	30
C*/methane	1070	47	40
C*/propane	2810	37	30

[a] Results in brackets were obtained after experiments.

The BG model, however, effectively initiates the flame later on in the explosion and thus fails to predict the time of peak overpressure.

Figs. 11 and 12 show a comparison of the peak overpressures at all the transducer positions. Fig. 11 provides all the data. Fig. 12 is restricted to experimental overpressures below 1 bar which, in common with the medium-scale experiments, show substantially higher predictive accuracy for experiments with peak overpressures up to the nominal value of 1 bar. In fact, all of the models provide very close agreement to the test result for the case of obstacle type E with methane, and consistently overpredict for propane. For the FLACS, COBRA and EXSIM codes the biggest differences between the model predictions and the experimental results occur for obstacle type C* with propane which yielded the highest peak overpressure. In the case of the REAGAS code the biggest difference occurs for obstacle type C* with methane. This overestimation of the overpressure demonstrates the, already mentioned, limitations of subgrid obstacle representation and the turbulent combustion model, applied in the REAGAS code at the time.

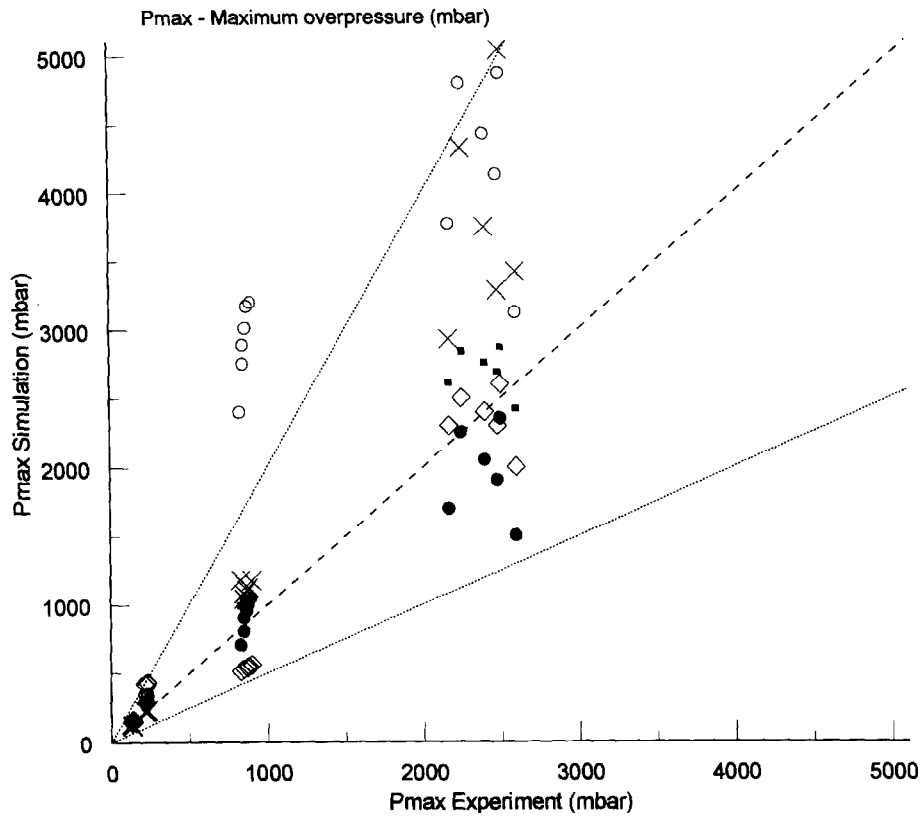

Fig. 11. Comparison of experiment and simulation for MERGE large-scale experiments (BG, Tel-Tek, CMR, PML). (×) COBRA predictions, (◇) EXSIM predictions, (●) FLACS predictions, (○) REAGAS predictions. Simulated maximum overpressure and experimental maximum overpressure (mbar).

The point is that the large-scale C* obstacle geometry can be considered in two ways:

(1) as equal to the medium-scale C geometry, extended with another 5 rows of obstacles to each side,

(2) as equal to the medium-scale A geometry, whose proportions are scaled up by a factor of 2.

Calibration of the C* simulation as an extended medium-scale C experiment resulted in the overestimation of the pressure as mentioned. If, on the other hand, the C* simulation was calibrated as a scaled up geometry A, the results overestimate the experimental data only slightly and were quite in line with the general trend. (Average overpressures for C* methane and propane would be 1030 and 2700 mbar respectively. Results were obtained after performance of experiments. Table 6 shows these values in brackets.)

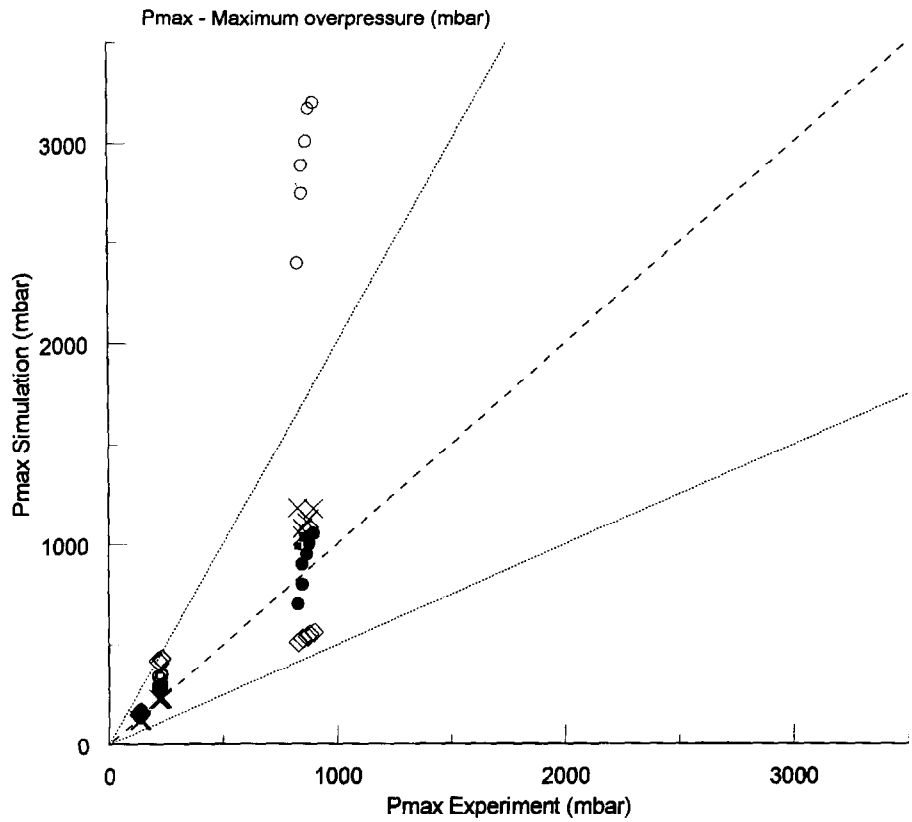

Fig. 12. Comparison of experiment and simulation for MERGE large-scale experiments with peak overpressures below 1 bar (BG, Tel-Tek, CMR, PML). (×) COBRA predictions, (◇) EXSIM predictions, (●) FLACS predictions, (○) REAGAS predictions. Simulated maximum overpressure and experimental maximum overpressure (mbar).

The predicted duration also varied greatly. However, the trends appear to be well predicted, showing smaller durations for higher peak overpressures. The predicted durations were roughly within a factor of two of those measured.

7. Discussion

The verification study which involved comparison of the predictions of the different models proved to be very constructive in demonstrating the correctness of implementation of the sub-models in the four codes. As a result of this exercise, any small differences in the implementation of the sub-models were immediately identified. In addition, the studies were also able to identify those sub-models which are most sensitive to the size of the computational grid cells, such as the turbulence and ignition sub-models. In the latter case the study demonstrated the necessity of having

sufficiently many cells in the reaction zone for the burning velocity to be predicted accurately.

All of the models gave accurate predictions of the pressure losses and turbulence production in simple non-reacting flows. There were, however, significant differences between the drag coefficients used and also the proportion of kinetic energy assumed to dissipate as turbulence. Even though all of the modellers referenced published material, it is clear that there is not a definitive opinion upon how the drag and turbulence models should be formulated. The later development and validation study also raised the question as to what extent flow development and flow acceleration effects should be taken into account. These have previously not been included in explosion models.

The enumeration and comparison of the turbulent combustion models proved valuable in quantifying their differences. This finding explained why there needed to be differences in the other sub-models for the codes to give general agreement with the experimental data. Thus, there are empirical aspects of the sub-modelling which can only be improved upon by further research.

It is nonetheless clear that the sub-modelling used in this study is at a sufficiently developed state for the codes to predict overpressures and durations reliably in these geometries for a large number of experimental conditions. The predictive accuracy degrades, however, when the overpressures are in excess of 1 bar, but the predicted overpressures still remain within a factor of two of the experimental value. This behaviour is readily explained by limitations in the combustion sub-models which have not been developed for application in the high-pressure regime when shocks are present.

It must be appreciated here that the model predictions of the large-scale explosion experiments were conducted prior to the experiments being conducted. This was done to allow the accuracy of the CFD-based explosion models to be independently assessed. All the explosion codes have subsequently been developed further and improved in their predictive capability for these experiments as a result of the total findings of the MERGE project and various other explosions projects.

8. Conclusions

A study has been conducted to investigate and improve the accuracy of four computational fluid dynamic (CFD) codes which are being developed for use on practical explosion hazard assessments. The codes are EXSIM (Telemark Technological Research and Development Centre), FLACS (Christian Michelsen Research), REAGAS (Prins Maurits Laboratory TNO) and COBRA (British Gas, Research and Technology). The study included comparison against exact numerical solutions, explosion experimental data and the results of fully resolved calculations using the GEISHA code (Imperial College of Science, Technology and Medicine).

The codes have a common mathematical basis but employ different numerical methods. The EXSIM and REAGAS codes employ first-order fixed finite-volume grid techniques. FLACS employs a second-order technique for flame tracking. COBRA is

fully second-order and uses a nodal embedding adaptive grid technique. GEISHA uses a second-order scheme and a fixed grid.

The most important aspect of practicable explosion models are the physical sub-models which describe the processes that are below resolution on affordable computational grids. The most important of these are the flame model, in particular the turbulent combustion model, and the drag and turbulence models.

A verification exercise, involving comparison with exact solutions, successfully demonstrated the accuracy of all of the codes but also identified differences between the combustion, drag and turbulence models. These differences arise even though all the contributors reference published material in support of their modelling assumptions. In the absence of a unified approach to the fundamental modelling assumptions the sub-models retain a level of empiricism.

The model development phase was successful in achieving good overall agreement with the small- and medium-scale experimental results. In order to achieve agreement with experiment, however, some sub-models needed further development beyond those used in the verification exercise. The high predictive accuracy for peak overpressure and impulse lessened, however, for those cases which yielded explosion overpressures in excess of 1 bar. The same overall result was true for the simulations of the large-scale experiments. This was attributed to the inability of the sub-models to describe the physical processes when strong shocks are present.

Further work is necessary in order to establish a unified approach to the sub-models used in this type of explosion code. The principle objective of such work should be to resolve the uncertainties in the physics of the combustion, drag and turbulence sub-models.

Acknowledgements

This research was co-sponsored by the CEC under the STEP Major Technological Hazards Programme (CEC contract: STEP-CT-0111 (SSMA)).

References

[1] B.H. Hjertager, Combust. Sci. Technol., 27 (1982) 159.
[2] J.R. Bakke, Numerical simulation of gas explosions in two-dimensional geometries, Ph.D. Thesis, Faculty of Mathematics and Natural Sciences, University of Bergen, August 1986.
[3] A.C. Van den Berg, REAGAS – A code for numerical simulation of reactive gas dynamics in gas explosions, Report No. PML 1989-IN48, TNO Prins Maurits Laboratory, 1989.
[4] W.P.M. Mercx et al., Modelling and experimental research into gas explosions, Overall Report of the MERGE Project, CEC contract: STEP-CT-0111 (SSMA), 1994.
[5] B.H. Hjertager, Modelling Identification Control, 5 (1985) 211.
[6] S.A.E.G. Falle, Mon. Not. R. Astr. Soc., 250 (1991) 581.
[7] S.V. Patankar, Numerical Heat Transfer and Fluid Flow, McGraw-Hill, New York, 1980.
[8] B. Van Leer, J. Comput. Phys., 14 (1974) 361.
[9] W.P. Jones and B.E. Launder, Int. J. Heat Mass Transfer, 15 (1972) 301.
[10] S.A.E.G. Falle and J.R. Giddings, in: K.W. Morton and M.J. Baines (Eds.), Proc. IFCD Conf. on Numerical Methods for Fluids, 7–10 April 1992.

[11] T. Hulek and R.P. Lindstedt, Adapting van Leer's limited antiflux method for the PISO algorithm for solving reacting turbulent flows, Fluids Section Report No. FL/91/26. Department of Mechanical Engineering, Imperial College of Science, Technology and Medicine, 1991.
[12] R.I. Issa, J. Comput. Phys., 62 (1986) 40.
[13] C.J. Geankoplis, Transport Processes and Unit Operations, Allyn and Bacon, Newton, MA, 2nd edn., 1983.
[14] VDI-Wärmeatlas, Berechnnungsbl. für d. Wärmeübergang, Hrsg. Verein Dt. Ingenieure-Düsseldorf.
[15] T.T. Kao and S.M. Cho, A numerical solution method for the prediction of flow and thermal distribution in shell-and-tube heat exchangers, ASME Paper No. 79-HT-63, 1979.
[16] Engineering Science Data Unit (ESDU), Crossflow pressure loss over banks of plain tubes in square and triangular arrays including effects of flow direction, Item Number 79034, April 1980.
[17] C.A. Catlin and R.P. Lindstedt, Combust. Flame, 85 (1991) 427.
[18] C.J. Rallis and A.M. Garforth, Progr. Energy Combust. Sci., 6 (1980) 303.
[19] B.F. Magnussen and B.H. Hjertager, Proc. 16th Int. Symp. on Combustion, The Combustion Institute, Pittsburgh, 1976, pp. 719–729.
[20] R.P. Lindstedt and V. Sakthitaran, 8th Symp. on Turbulent Shear Flows, Paper 22-5, TV Munich, 1991.
[21] T.D. Butler, J.K. Cloutman, J.K. Dukowich and J.R. Ramshaw, Progr. Energy Combust. Sci., 7 (1983) 293.
[22] B.J. Arntzen, Final report on modelling in MERGE, Christian Michelsen Research Report No. CMR-93-F25042, 1993.
[23] B.H. Hjertager, Numerical Simulation of Turbulent Flames and Pressure Development in Gas Explosions, Fuel–Air Explosions, SM Study No. 16, University of Waterloo Press, Waterloo, Canada, 1982, pp. 407–426.
[24] K.N.C. Bray, Proc. Roy. Soc. Lond., A431 (1990) 315.
[25] R.G. Abdel-Gayed and D. Bradley, Combust. Flame, 76 (1989) 213.
[26] R. Courant and K.O. Friedrichs, Supersonic Flow and Shock Waves, Interscience, New York, 1948.
[27] D.J. Tritton, Physical Fluid Dynamics, Oxford University Press, Oxford, 1988.